Effects of Iterative Spatial Filtering on DEM Data Structure

Andrew J. Stauffer[1], Barbara P. Buttenfield[1], and Lawrence V. Stanislawski[2]

[1] Department of Geography, University of Colorado, Boulder, Colorado USA
Email: astauffer@colorado.edu, babs@colorado.edu

[2] Center for Excellence in Geospatial Information Science (CEGIS),
United States Geological Survey (USGS), Rolla, Missouri USA
Email: lstan@usgs.gov

ABSTRACT: Digital Elevation Models (DEMs) are available with increasingly fine resolution. Many projects require some type of terrain generalization. Terrain must be visually clear and also integrate with other data (potentially generated at other resolutions). This project explores spatial filtering of DEM data drawn from various landscape types for the purpose of visual display. As data are gradually smoothed, the resolution can be assumed to change, but its rate of resolution change is unknown. This study iteratively filters DEM data in four study areas. After about 20 filtering iterations, the terrain data does not continue to drastically change and elevation values approach a state of homogenization.

KEYWORDS: DEM, generalization, resolution, spatial filtering

Introduction

Terrain is one of the most frequently included data layers in GIS spatial analysis. It is commonly used as an element for base mapping to represent macro-scale landforms. Terrain also is an important data layer for analytic purposes. It can be used to model runoff and stream flow, to predict sediment deposition, and for modeling habitat. Terrain derivatives, such as slope, curvature, and aspect, can support climate predictive models that use local and global orographic characteristics. Digital terrain also can be applied to anthropogenic development, such as cases of identifying acceptable building sites and identifying road construction through a landscape.

The terrain requirements for such projects range from geographic footprints that span several hundred square meters to the entire globe, and from fine to coarse resolution. For the largest scale projects, finer resolution elevation data are often needed, which requires airborne or field collection, often in the form of LiDAR. Many uses require coarser resolution than what is originally collected in available data. To accommodate the need for coarser resolution, digital terrain is generalized to improve processing times and data integration, and to facilitate human perception of data patterns.

"Generalization refers to any modification of detail in spatial information. It can involve reduction of geometric detail, classification to modify attribute details, or exaggeration to systematically introduce details as in smoothing, interpolation, or filtering" (Buttenfield and Mark, 1991). Data generalization is a common practice in the fields of GIS and cartography. Several controls on generalization include data purpose, data complexity, and scale reduction (Slocum et al., 2009; Robinson and Sale, 1969).

Several raster generalization methods have been identified and include spatial filtering, resampling, interpolation, and heuristic methods. All of these methods involve altering resolution explicitly (as in resampling and interpolation) or implicitly (as in filtering and heuristic methods). Implicit resolution changes produce a grid that maintains the source X, Y cell size while making the elevation attributes coarser and more simplified by reducing detail. It is important to generalize to appropriate resolutions and maintain data consistency.

This study examines how raster data are altered through implicit resolution change via iterative (repetitive) spatial filtering, and analyzes the rate of data change (resolution, terrain roughness) and how this varies across landscape types. This will be measured by examining changes in z-values, autocorrelation, and fractal dimension. Eight 7.5-minute quadrangles of 1/9-arc-second digital elevation data from flat and rugged landscapes in humid areas of the United States repeatedly are filtered through a focal mean process, and the change in the variation of the data is evaluated for each iteration through several metrics. Some background descriptions of the data and techniques used for this study are presented, followed by a discussion of results.

Background

The National Elevation Dataset

Data utilized in this project are part of the National Elevation Dataset (NED), a fine resolution, seamless, national coverage product developed by the U. S. Geologic Survey (USGS) (Gesch, 2007; Gesch et al., 2002). The NED project began in the 1970's and was designed to have a 30-meter spatial resolution. As time passed, the NED was refined to 1/3-, 1-, and 2-arc-second resolutions (or about 10-, 30-, and 60-meter resolutions, respectively). In 1999, full U.S. coverage of 1-arc-second data was completed and in 2002, 1/3-arc-second (about 10m) resolution began construction to conform to vertical and horizontal accuracy standards (U.S. Geological Survey, 1999). The datasets were derived from photogrammetric and Digital Line Graphic (DLG) interpolations methods and are now edited for hydrological enforcement rules to improve data integration (Osborn et al., 2001). The NED currently is being updated to 1/9-arc-second (about 3m) resolution but is not yet available for the entire conterminous United States (Gesch et al., 2002). 1/9-arc-second data are derived by LiDAR and IFSAR remote sensing methods which, because of the finer resolution, are not hydrologically enforced.

Comparing scale to resolution

With access to finer resolution datasets, a question arises, specifically which DEM resolution is appropriate for integrating existing vector datasets at a given mapping scale? Kimerling (2011) offers an equation to determine the appropriate DEM cell size (in ground units) for a given mapping scale, constrained by display pixel density. The output is designated for computer screen display. Alternatively, Tobler (1988) poses a similar mathematical formula that calculates the detectable resolution, the smallest object on the map that is expected to be identifiable at a given scale. The goal is to determine an appropriate resolution for integration between two datasets.

Although these formulas can be useful in suggesting appropriate scales in which data should be used, they do not completely answer the question of DEM resolution. Both "solutions" assume homogeneous data characteristics, which is rarely true. Additionally, terrain resolution must be adequate (i.e., not appear too sharp or blurry) while also integrating vertically with other data layers (e.g., hydrography, road networks) (Imhof, 2007). Depending on landscape characteristics (aridity, terrain roughness, etc.), different resolution data may be required.

Methods of terrain generalization

Common GIS techniques used to generalize terrain include spatial filtering, interpolation, and heuristic methods (structure recognition) (Weibel, 1992). All four methods have been researched extensively (e.g., Usery et al., 2004; Burrough and McDonnell, 1998; Brassel and Weibel, 1988) for cartographic display and analytical needs.

Weibel (1992) reviews several methods of terrain generalization. Spatial filtering commonly is used for minor scale reductions or for low-relief terrain. Spatial filtering redefines a cell value by performing a statistical transformation, commonly through calculation of focal mean elevation. Filtering methods include selective filtering, resampling, and global filtering. Selective filtering is useful for transitional terrain (mixed low-to-high relief), and in removing minor details while preserving important landscape features. Resampling can be effective for larger scale reductions or more rugged terrain; however, if the scale reduction is too great, resampling can ruin derived topological relations. Global filtering can be effective for minor scale reductions or for flat terrain because it smooths the data. Interpolation creates a surface from structure points (spot heights and benchmarks) that are extracted from finer resolution data. Heuristic generalization extracts a hierarchy of ridges and valleys, and interpolates the terrain based on these extracted features.

Each terrain generalization method is useful in its own way but all have pitfalls. Spatial filtering generalizes raster data gradually by focusing on a small focal neighborhood. If the focal window is too large, small features will be overpowered by global characteristics. Filtering preserves derived topology but only can be used for small scale changes; it also reduces local maxima and increases local minima. Resampling can generalize terrain aggressively but can easily corrupt derived topology. This can be problematic for spatial analysis, where topology and accuracy are paramount. Interpolation can preserve critical features and convert raster terrain into a triangulated irregular network (TIN). Data reduction through TINs greatly improves processing time and reduces file size, but can create artifacts within the data from the triangulation process. Heuristic methods are not commonly used for model generalization because of the intrinsic nature that the generalizations are not occurring within a statistical threshold (Weibel, 1992); however, generalization of structure lines can improve graphic clarity of a terrain by emphasizing specific features. It was noted at the outset that best practice advises against generalization of hillshades, emphasizing the importance of filtering the underlying terrain and reproducing the hillshade for display at smaller scales.

Methodology

Study areas

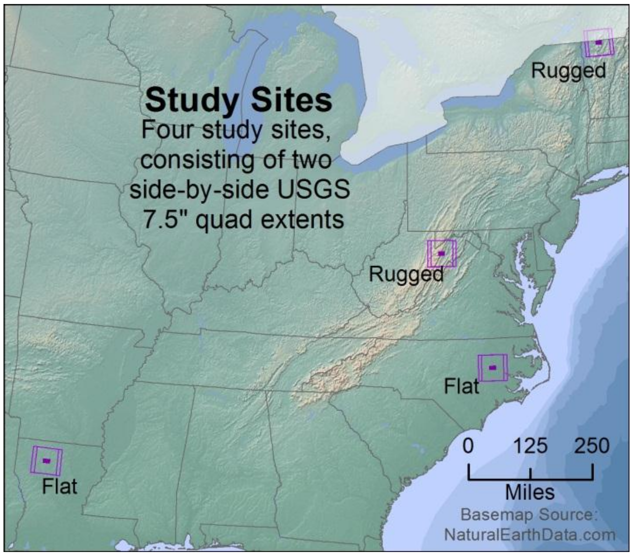

Figure 1: Eight study sites were chosen for this project including four in flat areas and four in rugged areas.

This project will examine progressively filtered data for four study areas in two physiographic settings (Figure 1). Landscape characteristics have been defined in terms of three terrain roughness characteristics and eight surface hydrographic characteristics) (Stanislawski et al., in press). Classifying these factors defines seven landscape types; this project will examine two of these landscape types including humid-rugged and humid-flat terrain. The four study areas were chosen with an extent of a USGS 7.5-minute quadrangle because some artifacts still exist within the NED from the original DLG compilation of the DEMs. Study areas include North Carolina and Louisiana (flat terrain), and West Virginia and Vermont (rugged terrain). For consistency, two side-by-side quads were chosen in each study area, producing eight study sites (Figure 2).

The study reported here is constrained by data availability because 1/9-arc-second data are not yet available for the entire United States. The intention in this research is to use three benchmark DEMs (bDEMs) at 1/9-, 1/3-, and 1-arc-second resolution, providing an available resolution range of about 10x. The study will filter the 1/9-arc-second bDEM. The generalized versions will be referred to as test DEMs (tDEMs).

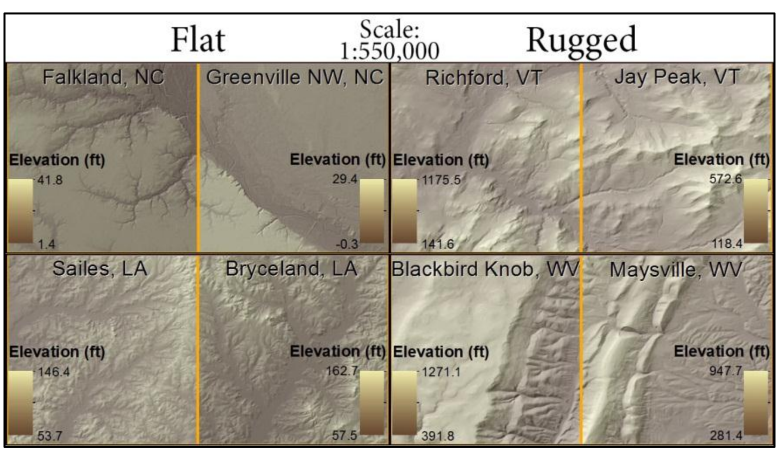

Figure 2: The eight study sites chosen for this project are grouped into two categories of flat and rugged terrain. Each of these categories has two study areas to evaluate similarity within the classification. Each study area contains two study sites with extents of a USGS 7.5-minute quad boundary.

Data processing

A 3x3 mean focal window was used to smooth and filter the 1/9-arc-second bDEM. The filtered tDEM was then input to subsequent filtering routines, continuing through 100 iterations. Preliminary experimentation indicated that within 100 iterations, the DEMs approach homogeneity (elevation values flatten as the filtering approaches equilibrium).

Structure analysis (terrain roughness and complexity)

Mean and standard deviation statistics were calculated within each 3x3 focal window. A geostatistical analysis also was conducted by examining the spatial autocorrelation of cell values within the 3x3-cell focal window to which the filter is being applied. These measures were aggregated over the entire study area for each iteration to define terrain roughness and to identify changing global homogenization of the DEM. Moran's I measures how similar a cell is to its defined neighbors (in this instance, queens-contiguity). The autocorrelation also was calculated and averaged at the focal-window scale because the metric is scale dependent (Griffith 1987). A global Moran's I would usually be higher in magnitude because of the extremely large sample sizes of values, and more difficult to identify changes.

Because this study has a cartographic display driver (i.e., the generation of hillshades), a shaded relief hillshade data layer was rendered from each filter iteration. Layers were then reclassified into illuminated (class 1) areas or non-illuminated (class 2) areas for simplicity. Reclassified hillshades were then processed using FragStats 4.0 (McGarigal et al., 2012) to determine the number of patches within each class and the class fractal dimension.

Fractal dimension was computed as a perimeter-to-area ratio (Mandelbrot, 1982). One would expect that, as a DEM is filtered, the number of patches should decrease as areas are homogenized; the complexity of these patches should also decrease because detail is being removed through the filtering process. Fractal dimension determines how the complexity of the data is being changed though each filter iteration.

Results

The focal mean of all eight study sites differs greatly, depending on the average elevation for each location. All focal means decrease only slightly through filter iterations, but remain similar to the focal mean of the original 1/9-arc-second bDEM. The change in focal standard deviation (Figure 3) shows similar trends in all study areas. All study areas display trend slopes that level off at about 20 iterations. Logarithmic trend lines were fitted to all graphs, and have slopes that vary from -0.011 ln(x) to -0.014 ln(x) in three of the study regions. An exception is the North Carolina study site with a slope of -0.007 ln(x). Graphs additionally were compared to the coarser resolution bDEMs (Table 1), which, in all cases, were greater than any values encountered in any of the tDEMs.

Focal Moran's I graphs (Figure 4) demonstrate that all study sites stop exhibiting large jumps in autocorrelation after about 10 iterations. The maximum focal Moran's I values also level out at about 0.3 for all study sites. Exponential trend lines were fit to the curves to examine the graph lines. The rugged study areas had slopes that increase at a slower rate, which range from $x^{0.009}$ to $x^{0.029}$ compared to flat study areas that increase at rates of

$x^{0.007}$ to $x^{0.0003}$. Again, the graphs were compared to 3x3 focal Moran's I values generated from the coarser resolution bDEMs. In all cases, the Moran's I values from the coarse-resolution bDEMs were lower than any of the values present in the tDEMs; however, as resolution became coarser, the focal Moran's I values continued to decrease; this trend was opposite than what was observed through filter iterations.

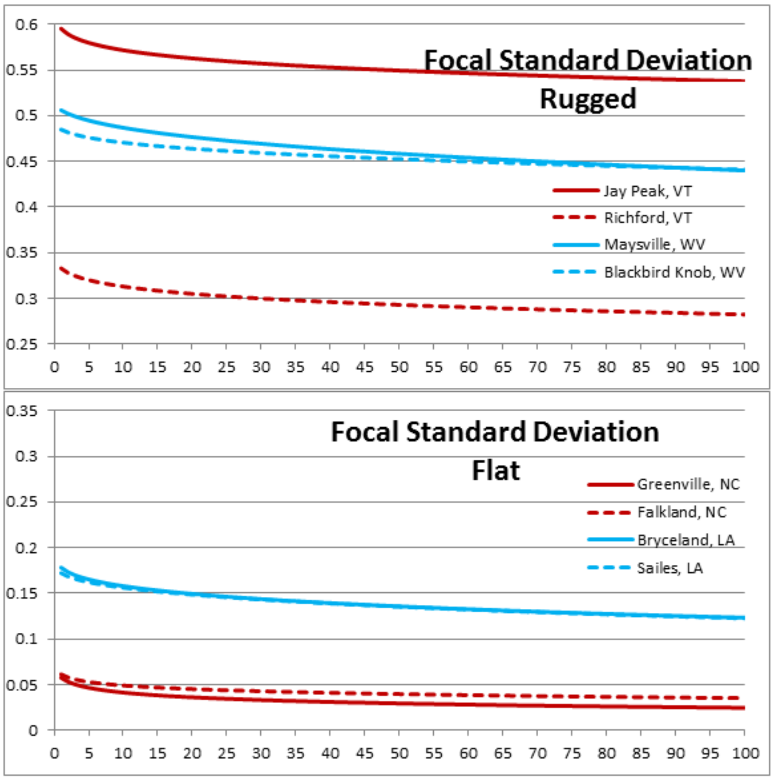

Figure 3: Focal Standard Deviation (y-axis) trends of all eight study sites though filter iterations (x-axis). Trends within paired quads for each study area are most similar. The exception here is the Vermont study sites, which is likely due to transitioning terrain roughness from mountainous to flat areas (See Figure 2).

Table 1: The focal Standard Deviations and Moran's I values of the coarser resolution bDEMs.

Study Site	*St. Deviation 1/3-AS bDEM*	*St. Deviation 1-AS bDEM*	*Moran's I 1/3-AS bDEM*	*Moran's I 1-AS bDEM*
Jay Peak VT	1.77	5.10	0.26	0.25
Richford, VT	0.99	2.77	0.24	0.22
Maysville, WV	1.50	4.27	0.27	0.24
Blackbird Knob, WV	1.44	4.16	0.27	0.26
Greenville, NC	0.15	0.34	0.13	0.06
Falkland, NC	0.17	0.41	0.17	0.12
Bryceland, LA	0.52	1.34	0.21	0.17
Sailes, LA	0.50	1.33	0.22	0.18

As one output of the FragStats 4.0 processing, the total number of patches was calculated for each filter iteration. Patches were defined as a cluster of cells within a hillshade that was either more or less than 50% illuminated. In all cases, the number of patches decreased exponentially through increasing filter iterations. Table 2 compares the start and end counts of patches for each study site, as well as patch counts for coarser resolution bDEMs. In all flat study areas, the total number of patches in the tDEMs was equal to coarsest resolution bDEM. This condition frequently was met before 30 iterations. Only one of the study sites (Richford, VT) in the rugged study areas met this condition, which occurred at the 90th filtering iteration.

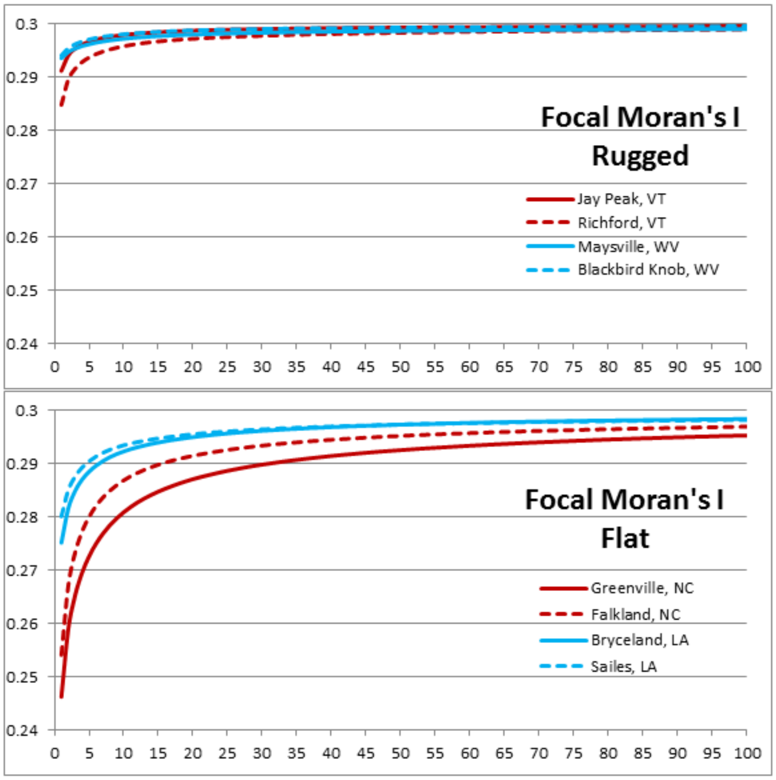

Figure 4: Focal Moran's I (y-axis) trends of all eight study sites though filter iterations (x-axis). Trends are similar through all study sites, but the flat study areas have a faster change rate.

Table 2: The count of patches for the tDEMs and bDEMs

Study Area	*Total Patches 0th iteration*	*Total Patches 100th iteration*	*Total Patches 1/3-AS bDEM*	*Total Patches 1-AS bDEM*
Jay Peak VT	19188	366	2798	348
Richford, VT	9124	161	1415	182
Maysville, WV	6458	620	1939	381
Blackbird Knob, WV	5612	687	1520	293
Greenville, NC	1042	1	61	1
Falkland, NC	485	1	21	1
Bryceland, LA	1540	1	108	1
Sailes, LA	744	2	39	2

The changes in fractal dimension through filter iterations are more complex than other statistical measurements (Figure 5). In the flat study areas, patches homogenize into only one class before the 100th filter iteration and thus a fractal dimension could not be computed for the other class. Overall, the rugged study areas consistently have more complex patch shapes than flat study areas. The trends on all the graphs display fluctuations, which likely is due to cells changing classes through the filter process; however, the continual fluctuation is unexpected and results were anticipated to be much more like that of Jay Peak, VT, which is the only site that continually decreases in patch complexity.

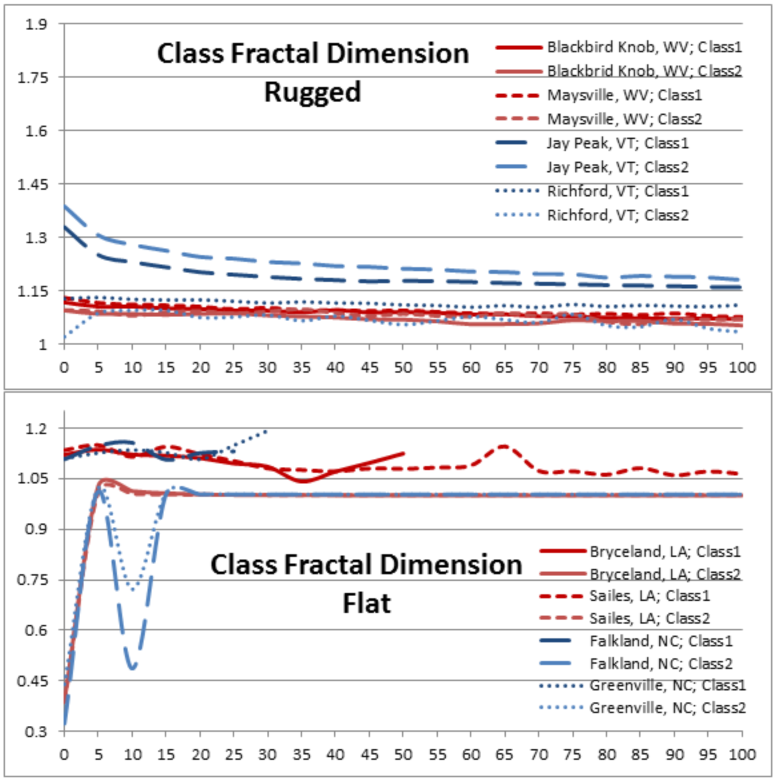

Figure 5: Fractal Dimension (y-axis) trends of all eight study sites though filter iterations (x-axis). Class 1 represents cells that would be illuminated in the analytical hillshade and class 2 represents cells that would not be illuminated.

Due to noise in the fractal dimensions, it is difficult to confirm similarity to coarser resolution bDEMs (Table 3). When the bDEM fractal dimensions intersect the tDEM values, it occurs after many filter iterations and the tDEM trends often intersect the bDEM values several times. The only outlying study site that does not intersect bDEM fractal dimension value is Jay Peak, VT, which has a greater fractal dimension than any other study site. In the flat study areas, 3 of 4 study sites have class 2 fractal dimension trends that level off at a value of 1.003 after 20 iterations. This is because these sites have homogenized into 1-class landscapes by this point.

Table 3: Fractal Dimensions of hillshade classes derived from coarser resoluion bDEMs. Class 1 is cells that are greater than 50% illuminated and class 2 is cells that are less than 50% illuminated.

Study Area	*Class 1 FD 1/3-AS bDEM*	*Class 1 FD 1-AS bDEM*	*Class2 FD 1/3-AS bDEM*	*Class 2 FD 1-AS bDEM*
Jay Peak VT	1.081	1.064	1.063	1.046
Richford, VT	1.090	1.072	1.066	1.030
Maysville, WV	1.091	1.065	1.062	1.044
Blackbird Knob, WV	1.082	1.072	1.054	1.041
Greenville, NC	1.086	1.003	1.018	N/A
Falkland, NC	1.089	1.003	1.008	N/A
Bryceland, LA	1.075	N/A	1.023	1.000
Sailes, LA	1.095	1.069	1.010	1.001

Discussion

Several controls on generalization include data purpose, data complexity, and scale reduction. The generalization control of data purpose for this project was to generate an appropriate cartographic display (hillshade). This was evaluated by examining how data complexity changed through iterative spatial filtering to help identify a set of guidelines for displaying hillshades at a given scale. Because terrain characteristics are unique for just about every mapping project, this study evaluated the data complexity in four study areas, utilizing eight study sites. Two study areas were in rugged locations and the remaining two were in flat locations to examine how terrain roughness affects the generalization process.

The changes in focal mean across filtering iterations show promising results and are expected to deviate minimally from mean of the 1/9-arc-second bDEM. These changes will reflect the increasing local minimum and decreasing local maximum because of the smoothing process. If the focal mean changes too much, this would also be reflected in the visual output of the analytical hillshade. The purpose of iterative filtering is to gradually smooth the terrain without making drastic changes to the landscape.

The focal standard deviations show expected results. The standard deviation should gradually decrease as the nine focal cells are homogenized. In all cases, after about 10–20 filter iterations, the trends stabilize. This implies that further iterations would not simplify the terrain. The difference in standard deviations between the flat and rugged study areas likely is due to the terrain roughness characteristics and would closely be linked to the reasoning of why the focal means are so dissimilar. Because rugged study sites have a greater elevation range, the standard deviations will be greater. The fitted trend line [with a slope of -0.007 ln(x)] for North Carolina again is related to the small range of elevation values.

An unexpected result was the difference in focal standard deviation values of the tDEMs compared to the bDEMs. It was expected that comparing these values could lead into insights about when a tDEM was most similar to the next coarser resolution bDEM. The likely cause that this comparison was not able to be made was focal window was measured in cells, opposed to meters. The focal windows for all DEMs were 3x3 cells in size. This meant that the focal window was approximately 10x10 meters for the 1/9-arc-second tDEMs. The 1/3-arc-second bDEM had the same focal window, but was about 30x30 meters in size. This difference in linear size changes the scale at which the terrain (and landforms) is being analyzed and could bias results. Since this same pattern also was observed for the Moran's I comparison, the same explanation can apply. In the future, the bDEMs should first be processed and resampled (down-sampled) to have a linear resolution of 1/9-arc-second. This may allow for more comparable results since the focal windows will be comparing the same areas.

Although the Moran's I values in all study areas start at different values, the ending autocorrelation values is about 0.3 in all study sites. This is interesting because the results appear to not be affected by the landscape characteristics. However, the autocorrelation values increase to this level at a slightly faster rate in the flat study areas (about 10 – 20 filter iterations) opposed to rugged areas (about 15 – 25 iterations). This implies that flat study areas do not need to be filtered as many times to accomplish the same amount of generalization compared to more rugged areas.

It is also curious that the Moran's I values peak just under 0.3, when 1.0 represents a completely homogenous area. This could possibly be happening because spatial autocorrelation indices are scale dependent. A global Moran's I statistic for these study areas result in values close to 1.0, regardless of filter iterations. Since the number of cells in these study areas is quite large (approximately 4000x4000 for 1/9-arc-second DEMs), the autocorrelation results in much higher values. It is likely that after 10–25 filtering iterations, all of the 3x3 cell landforms have been homogenized to the point where they do not change. In the future, introducing a correlogram to the focal Moran's I calculations could provide more insight on how autocorrelated the study sites are becoming through filter iterations. Another way to reduce the scale dependencies of Moran's I would be by examining different sized focal windows.

The fractal analysis was not as insightful as anticipated. Due to the fluctuations in the data, no conclusive interpretations can be extracted. This could be for several reasons. First, the terrain derivative that was chosen (analytical hillshade) may not have been as appropriate as slope or aspect. Since the hillshade was generated from default settings (315° azimuth), landscape features that are aligned to 315° (running NW to SE) would be omitted from the shading. Finally, the even binary classification of illumination values may have included transitional (flat) zones that added additional noise to the output.

The variance in the fractal dimension results also is strange. It was promising to see the number of patches in flat study areas approach one, causing the fractal dimension to level off at 1.0. This implies that these study areas are able to be filtered adequately to meet the complexity values of the coarser resolution bDEMs; however, in many cases, this did not happen. The anticipated results were expected to be similar to that of Jay Peak, VT. Since the expected result occurred here, it adds strength to the possibility that the classification scheme used to create the classes simply was not adequate, or may require a unique testing scenario for each study site.

This study has shown that iteratively filtering DEM data with a 3x3 focal mean process behaves differently in flat regions compared to rugged regions in terms of rates of data change. Flat regions demonstrate faster rates of change in terms of data complexity with increasing filter iterations; however, it is also observed that the data stop changing drastically after about 10–20 iterations, regardless of terrain characteristics. More work still is required in relating this information to changes in resolution via comparisons to coarser resolution bDEMs (and thus how appropriate filtered data will be for different mapping scales). Additionally, the requirement of data integration still needs to be examined. This can be done by extracting flowlines from the generalized terrain datasets and comparing results to benchmark hydrographic data. This will provide insight into how the landscape structure is being altered by the generalization process.

Acknowledgements

The work of Dr. Buttenfield is supported by USGS-CEGIS grant #04121HS029, "Generalization and Data Modeling for New Generation Topographic Mapping".

References

Brassel, K. and Weibel, R. (1988) A Review and Conceptual Framework of Automated Map Generalization. *International Journal of Geographical Information Systems*, 2, 3, pp. 229-244.

Burrough, P., and McDonnell, R. (1998) *Principles of Geographic Information Systems*. London: Oxford Press.

Buttenfield, B., and Mark, D. (1991) Expert Systems in Cartographic Design in *Geographic Information Systems: The Microcomputer and Modern Cartography*, Taylor, D. (ed.). Elmsfor: Pergamon Press.

Gesch, D. (2007) The National Elevation Dataset in *Digital Elevation Model Technologies and Applications: The DEM Users Manual*, Maune, D. (ed.), 2ed. Bethesda, Maryland, American Society for Photogrammetry and Remote Sensing: pp. 99-118.

Gesch, D., Oimoen, M., Greenlee, S., Nelson, C., Steuck, M., and Tyler, D. (2002) The National Elevation Dataset. *Photogrammetric Engineering and Remote Sensing*, 68, 1, pp. 5-11.

Griffith, D. (1987) *Spatial Autocorrelation: A Primer*. Washington DC: Association of American Geographers.

Imhof, E. (2007) *Cartographic Relief Presentation*, 1ed. Redlands: ESRI Press.

Kimerling, J. (2011) DEM Resolution, Output Map Pixel Density, and Largest Appropriate Map Scale, *ESRI Mapping Center Blog*: http://blogs.esri.com/esri/arcgis/2011/02/28/dem-resolution-output-map-pixel-density-and-largest-appropriate-map-scale/ Last visited 8/12/12

Mandelbrot, B. (1982) *The Fractal Geometry of Nature*. New York: W. H. Freeman and Co.

McGarigal, K., Cushman, S., and Ene, E. (2012) FRAGSTATS v4: Spatial pattern Analysis Program for Categorical and Continuous Maps. Computer software program produced by the authors at the University of Massachusetts, Amherst. http://www.umass.edu/landeco/research/fragstats/fragstats.html Last visited 8/1/12.

Osborn, K., List, J., Gesch, D., Crowe, J., Merrill, G., Constance, E., Mauck, J., Lund, C., Caruso, V., and Kosvich, J. (2001) National Digital Elevation Program in *Digital Elevation Model Technologies and Application: The DEM Users Manual*, Maune,

D. (ed). Bethesda: American Society for Photogrammetry and Remote Sensing, pp. 83-120.

Robinson, A., and Sale, R. (1969) *Elements of Cartography*, 3ed. New York: John Wiley & Sons, Inc.

Slocum, T., McMaster, R., Kessler, F., and Howard, H. (2009) *Thematic Cartography and Geovisualization,* 3ed. Upper Saddle River: Pearson.

Stanislawski, L., Finn, M., and Buttenfield, B. (in press) Integrating Hydrographic Generalization Over Multiple Physiographic Regimes in *Generalization and Data Integration*, Buttenfield, B., and Mackaness, W. (eds).

Tobler, W (1988) Resolution, Resampling, and All That in *Building Data Bases for Global Science*, Mounsey, H. and Tomlinson, R. (eds.). London: Taylor and Francis, pp. 129-137.

Usery, L., Finn, M., Scheidt, D., Ruhl, S., Beard, T., and Bearden, M. (2004) Geospatial Data Resampling and Resolution Effects on Watershed Modeling: A Case Study Using the Agricultural Non-Point Source Pollution Model. *Journal of Geographical Systems*, 6, 3, pp. 289-306.

U. S. Geological Survey (1999) Map Accuracy Standards. US Department of the Interior and US Geological Survey, USGS Fact Sheet 171-99.

Weibel, R. (1992) Models and Experiments for Adaptive Computer-Assisted Terrain Generalization. *Cartography and Geographic Information Society*, 19, 3, pp. 133-153.